Measurement 42 (2009) 290–297

Contents lists available at ScienceDirect

Measurement

journal homepage: www.elsevier.com/locate/measurement

The electric and magnetic properties of Co and Fe films percept from the coexistence of ferromagnetic and microstrip resonance for a T-type microstrip

Yi-Chen Yeh [a], Jun-De Jin [b], Ching-Min Li [a], Juh Tzeng Lue [c,*]

[a] Institute of Photonics Technologies, National Tsing Hua University, Hsin Chu, Taiwan
[b] Department of Electronic Engineering, National Tsing Hua University, Hsin Chu, Taiwan
[c] Department of Physics, National Tsing Hua University, Kuang Fu Road, Section 2, No. 101, Hsin Chu 30042, Taiwan

ARTICLE INFO

Article history:
Received 28 December 2006
Received in revised form 25 February 2008
Accepted 19 June 2008
Available online 10 July 2008

Keywords:
Microwave microstrip
Structure mode resonance
Ferromagnetic resonance
Magnetic Co and Fe films

ABSTRACT

Ferromagnetic resonance for magnetic thin films is found to be coexisted with the transmission resonance of a T-type microwave microstrip at certain applied magnetic fields. The frequency dependence of conductivity, the magnetization, and the magnetic anisotropy of magnetic films can be eventually solved from the measured resonance frequency and quality Q factors of the resonance spectra. Equivalent resistances (R), inductances (L), and capacitances (C) corresponding to the displayed transmission S_{21} spectra are simulated to comply with proper values. With this equivalent circuit, an accurate determination of the magnetic properties can be closely scrutinized.

1. Introduction

The large demand in communication and video applications [1] intrigues us an impetus to develop the design of monolithic microwave microstrip circuits for the use of filters and resonators. Microwave techniques allow high sensitivity measurement of the dependence of the conductivity of thin magnetic films on frequencies, temperatures [2–4], and magnetic fields [5,6]. A permissive investigation on the resonance frequency tunable by magnetic or electric fields for filters is desired [5]. Measurement of the magnetic field dependence on resonant frequency shifts of the microwave microstrip has been performed by Tsutsumi and Tamura [6]. There have been a lot of studies on the measurement of the complex permeability over a broad frequency band [7]. The dynamic susceptibility deduced from ferromagnetic resonance spectra in magnetic films with a non-uniform magnetic configuration was reported [8].

In previous works we had reported the coexistence of ferromagnetic resonance (FMR) [9] and microstrip structure mode resonance (MSMR) [3] for cobalt films under magnetic fields from which we can eventually deduce the electric and magnetic properties of the magnetic films from the measured resonance frequency and the quality factor (Q) of the resonance spectra. There are 13 mode resonant lines within the input frequencies ranging from 0.5 to 40 GHz. Since the FMR of the magnetic films occurs even without an applied external magnetic field owing to the inherited internal anisotropic field, the deduction of physical constants merely arising from resonance frequencies and quality factors implies unexpected errors especially for those films intrinsically inherited with high anisotropic field. We have also studied in detail the magnetic domain walls by the magnetic force microscopy for various thickness of nickel and cobalt films [10].

* Corresponding author. Tel.: +886 35742551; fax: +886 35723052.
E-mail address: jtlue@phys.nthu.edu.tw (J.T. Lue).

0263-2241/$ - see front matter © 2008 Elsevier Ltd. All rights reserved.
doi:10.1016/j.measurement.2008.06.012

In this work, we describe equivalent circuits with prescribed 13 parallel resistance–inductor–capacitor (*RLC*) values deduced from the measured MSMR resonance frequencies and *Q* factors for each specified resonance line in series with the *RLC* deduced from a pure FMR. Even without applying magnetic field, the MSMR inevitably includes an accompanied FMR resonance by the inherited anisotropic field. The true resonance frequencies attributing to the independent FMR and MSMR can be separately retrieved from the equivalent *RLC* circuit. This method prevalently determines a much more accurate value of the magnetic constants of the film especially for those films behaving with high anisotropic field that affects the FMR frequency largely at zero applied fields.

2. The ferromagnetic resonance and T-type microwave microstrip resonance

Several planar transmission lines (e.g. stripling, ring, and T-junction) have been developed. In order to eliminate the air-gap problem for energy coupling and for the privilege of physical property studies of metal films at microwave frequencies, we endeavor to construct the microstrip T-junction. A T-type microwave microstrip is shown in Fig. 1 where the microwave field feeds from port 1 and outputs from port 2 of the main strip line, the magnet field is parallel to the side arm. A matched 50-Ω-transmission line depending on the thickness of the dielectric material, the effective dielectric constant, and the line width should be designed with the specified dimensions as derived from the reported works [9,11,12]. The microstrip structure mode resonance (MSMR) frequency ω_{res} occurs at

$$\omega_{res} = \frac{nc}{4(l + \Delta l)\sqrt{\varepsilon_{eff}(f)}}, \quad n = 1,3,5,7\ldots.. \tag{1}$$

where Δl is the additional length after taking into account of the effective length [13] of the open-ended stub representing a quarter-wave resonator. The quality factor *Q*, and the transmission coefficient S_{21} were defined in our previous work [3]. The surface resistance R_s, the dielectric effective constant of the substrate can be readily derived from the transmission coefficient S_{21} spectra measured by a HP 8722D vector network analyzer.

The magnetic moments of the thin film undergo a resonant absorption under an external microwave field that is in a direction perpendicular to the applied DC magnetic field H_0. The ferromagnetic resonance (FMR) manifests, For the T-type resonator, the microwave field absorbed in the side arm is largest when the arm length is an odd integer of the incident quarter-wavelength $\lambda_g/4$.

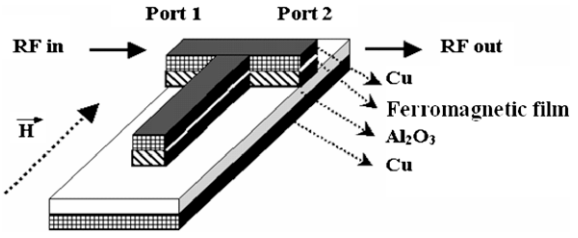

Fig. 1. A T-microwave microstrip. The layers are respectively copper, sapphire, ferromagnetic film (iron and cobalt), and copper as counted from bottom.

This FMR coexists with the MSMR at a resonance frequency of

$$\omega = \gamma\sqrt{(H_o + H_a) * (H_o + H_a + \mu_0 M_s)}, \tag{2}$$

where $\gamma = e/m$ is the gyromagnetic ratio, H_a is the anisotropic field depending on the crystal symmetry and orientation and M_s is the saturated magnetization. The FMR resonances are existed even the applied field H_0 vanishes. Here we have implied the demagnetizing factor for an infinite plane of thin film to be $N_x = N_z = 0$, $N_y = 4\pi$ as the external magnetic field lies on the *xz* plane.

3. Models of resonance circuits

As formulated in Eq. (2), the FMR occurs even without an external field H_0 owing to the inherited internal anisotropic field resulting in an introduction of errors to determine the physical constants as extruded from the measured MSMR. The errors can be eliminated by simulation the measured resonance frequencies and the *Q*-values of several MSMR spectra for parallel equivalent *RLC*s at high magnetic fields beyond the occurrence of FMR. For pure FMR, a series equivalent *RLC* circuit can also be deduced from the experimental data. The true resonance FMR frequencies at various external fields are crucially depended on the anisotropic field, which can be evolved from the simulated equivalent circuit. There are three resonant modes occurring in the T-type resonator. The first is the FMR relevant to the main strip line that is equivalent to a series resonator connected in parallel to the system Z_{in}. The second is the MSMR of the T-resonator that is equivalent to a series resonator connected in parallel to the system. And the third is the FMR related to the side arm that is equivalent to a series resonator connected in parallel to the MSMR of the side arm. The equivalent circuit and the input impedance of the side arm are shown respectively in Fig. 2(a) and (b).

We shall express that the series and parallel *RLC* resonators have the same transmission response at resonant frequency. The series resonator as shown in Fig. 3 has a *Q* factor as

$$Q = \omega_0 \frac{2W_m}{P_{loss}} = \frac{\omega_0 L}{R} = \frac{1}{\omega_0 RC}, \tag{3}$$

where $2W_m$ is the electromagnetic energy stored in the circuit, P_{loss} is the power dissipated and $\omega_0 = 1/\sqrt{LC}$ is the resonance frequency.

The input impedance is at a minimum as expressed by the equation

$$\begin{aligned} Z_{in} &= R + j\omega L\left(1 - \tfrac{1}{\omega^2 LC}\right) = R + j\omega L\left(\tfrac{\omega^2 - \omega_0^2}{\omega^2}\right), \\ &\approx R + j2L\Delta\omega \approx R + j\tfrac{2RQ\Delta\omega}{\omega_0}. \end{aligned} \tag{4}$$

In case of parallel resonators, the equivalent circuit is shown in Fig. 4 by which the input impedance is calculated as

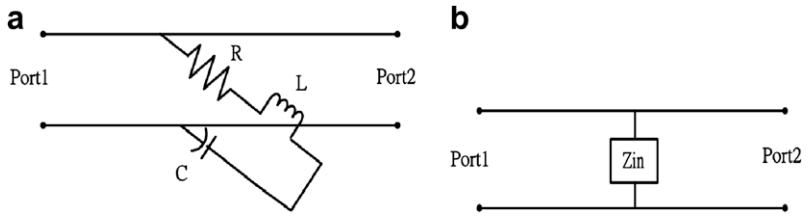

Fig. 2. The equivalent circuit for a T-type microstrip resonator: (a) equivalent *RLC* of the side arm and (b) the input impedance looked into the side arm.

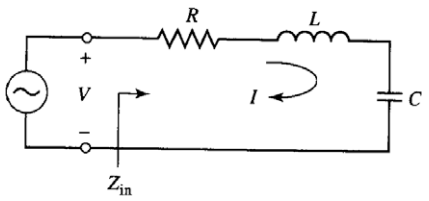

Fig. 3. The series *RLC* circuit representing the MSMR and FMR.

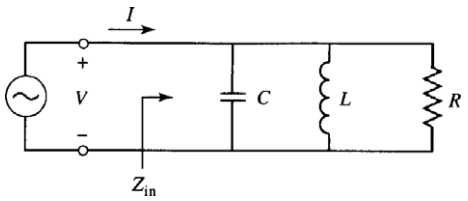

Fig. 4. The equivalent circuit of a parallel resonator representing the FMR.

$$Z_{\text{in}} = \left(\frac{1}{R} + \frac{1}{j\omega L} + j\omega C\right)^{-1} \approx \frac{R}{1 + 2j\Delta\omega RC} = \frac{R}{1 + 2jQ\Delta\omega/\omega_0}, \quad (5)$$

The impedance $Z_{\text{in}} = R$ is maximum at resonance with $\Delta\omega = \omega - \omega_0 = 0$. The transmission coefficient S_{21} for the FMR series resonator connected in series circuits as shown in Fig. 3 and the FMR parallel resonator connected in parallel circuits as shown in Fig. 4 have similar frequency responses as shown in Fig. 5(a) and (b), respectively.

On the other hand, the parallel FMR resonator connected in parallel to the MSMR circuit and series resonator connected in series also has similar frequency responses as shown in Fig. 7. Similar results of S_{21} as shown in Figs. 6 and 7 suggest us that the series and parallel resonators can be interchanged with equivalent transmission response.

4. Experiment results and discussion

In order to observe the coexistence of the MSMR and the FMR, a T-microstrip resonator of magnetic films was constructed. The shadow mask lithography was exploited to fabricate the T-microstrip resonator. Cobalt and iron films of thickness of 2–5 μm were thermally evaporated on (0001) sapphire substrates with a stainless-steel mask of thickness $h = 0.5$ mm under a vacuum pressure of 10^{-4} Pa. The backside of the sample was vacuum deposited with copper film. The reflectivity S_{11} and transmission S_{21} parameters were measured by an HP 8722D network analyzer with the microstrip attached by a universal test fixture which is installed at the center of an electromagnet. The calibration kits carry out the full two-port calibration procedures.

To verify that the variation of the transmission spectra S_{21} with applied magnetic field is attributed to the

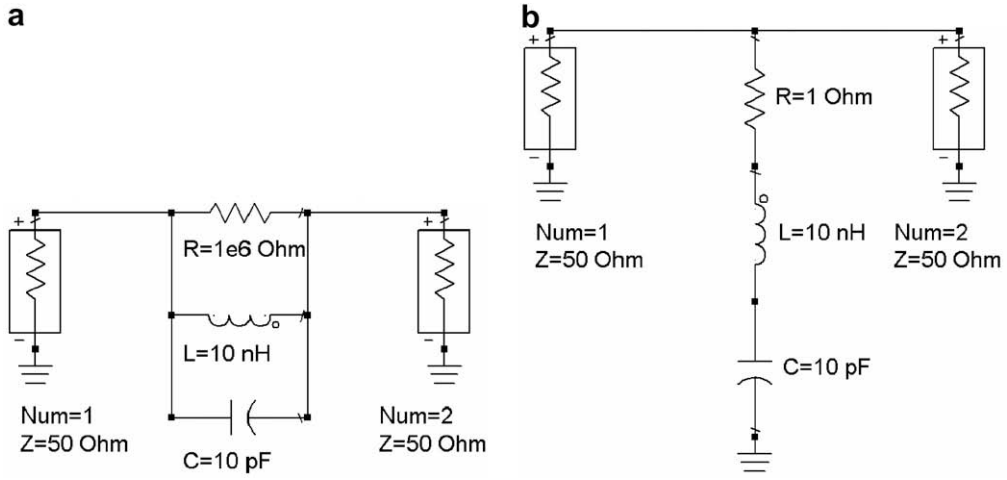

Fig. 5. Circuits for (a) series resonator connected in parallel circuit and (b) parallel resonator connected in series circuit.

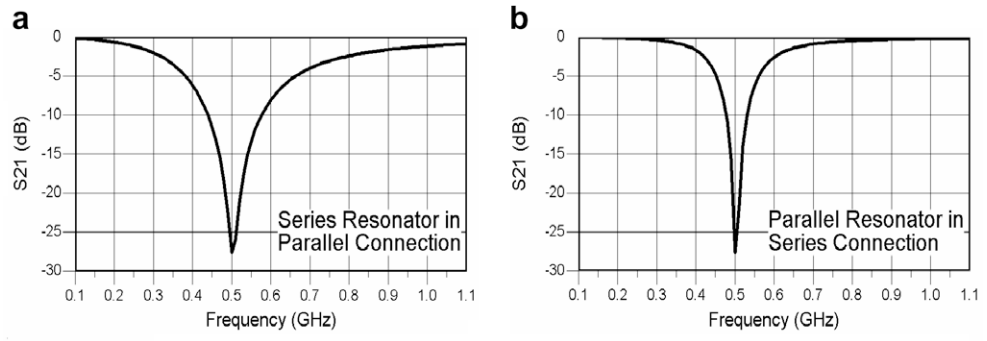

Fig. 6. Frequency response of S_{21} for above circuits.

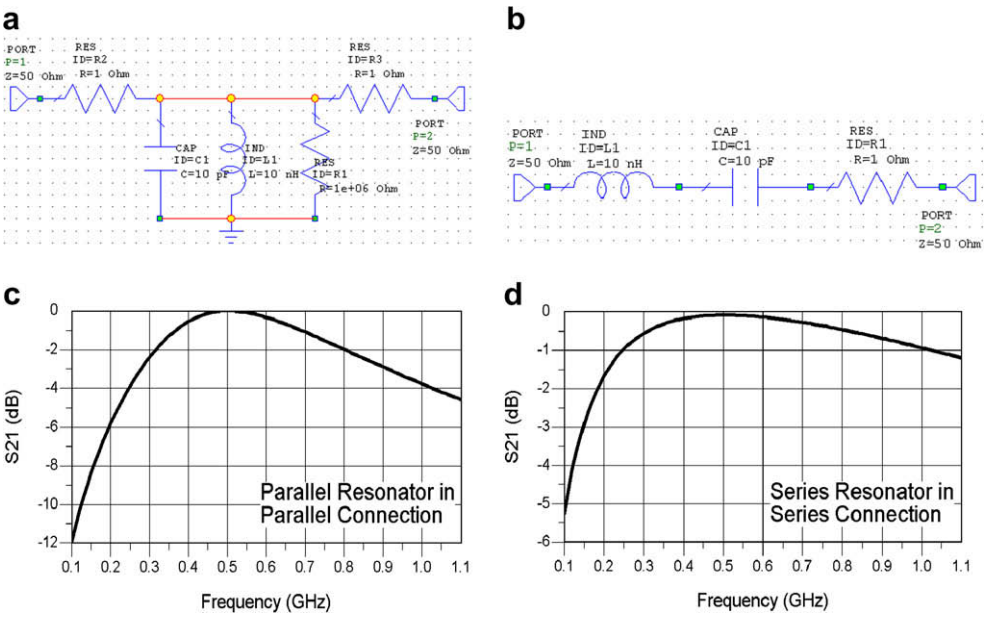

Fig. 7. Circuits for (a) the parallel resonator connected in parallel circuit, (b) the series resonator connected in series circuit, and the frequency response on S_{21} (c) for (a) circuit, and (d) for (b) circuit, respectively.

ferromagnetic property and not to the magnetoresistivity, we have plotted curves, which are deducted from the two measured spectra with and without applying a magnetic field on films deposited of silver, copper, and iron respectively as shown in Fig. 8. Obviously null changes of curves for microstrips constructed from non-magnetic metal films are found, whilst the subtracted S_{21} spectra of the iron microstrip changed much apparently when the magnetic field was applied.

The FMR manifests during the structure mode resonance at then the microwave field feeds into the side arm of T-microstrip being maximum. There are eleven transmission S_{21} spectra for the T-microstrip within frequencies range of 0.5–40 GHz. Fig. 9 demonstrates that the position of the magnified fifth resonant-dip of the iron microstrip shifts with the magnetic field in a loop rotate in counter-clockwise direction. Fig. 10(a) and (b) represent the variations of the Q and attenuation factors with magnetic fields at different resonant frequencies, which intimately follows the occurrence of FMR. Fig. 10(c) shows the dependence of surface resistivity on magnetic fields at different resonance frequencies. In the ballistic transport system where the electron mean free path is longer than the thin film thickness, the electron scattering with boundaries plays the essential role in conduction. The cyclotron motion of electrons in the magnetic field reduces the scattering with surfaces resulting in decreasing the resistivity. As the frequency of incident electromagnetic field increases, the ballistic transport becomes diffusion transport where the collision increases due to the high alternating current. If the skin depth δ is much larger than the mean free path l with $l \gg v/\omega = \xi$, where ξ is the pitch of the cyclotron orbit, wherein the l decrease at low

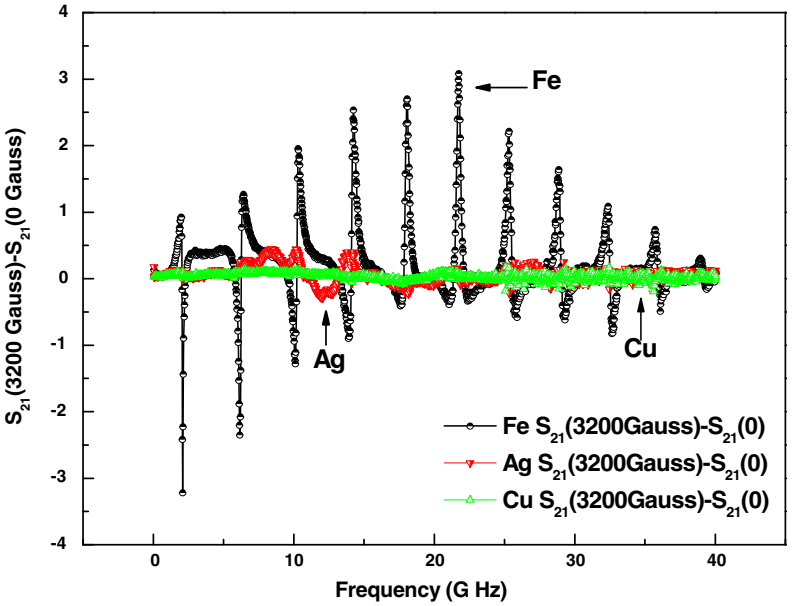

Fig. 8. Curves representing the subtraction of the spectra measured separately, with and without an applied magnetic field for silver, copper, and iron, respectively.

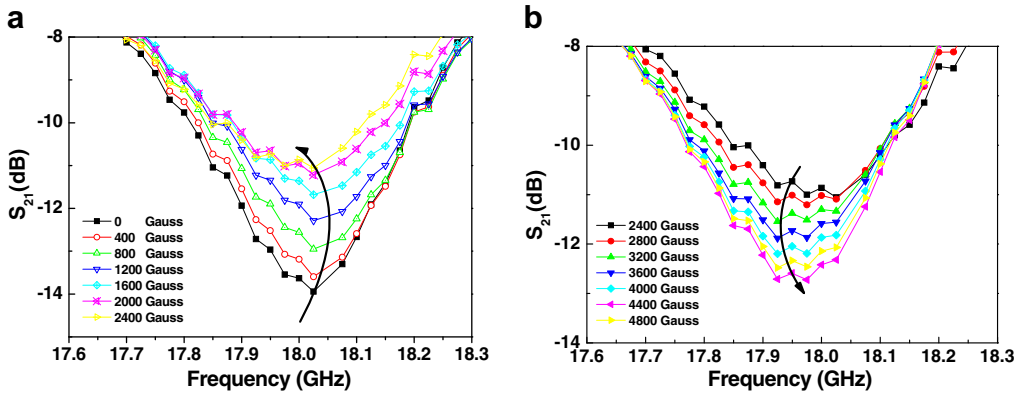

Fig. 9. The transmission spectra of the fifth structure-mode of the iron T-microstrip under various magnetic fields illustrating that the resonance dips (a) increase with magnetic fields, and (b) decrease with magnetic fields. The heavy curves are the guide lines for viewing the shift of the resonance dips.

magnetic field and then increases by the reduction of collision with the surface.

The FMR resonant frequencies at various magnetic fields are shown in Fig. 11. For iron films, the demagnetization factors are $N_x = 4\pi$ and $N_y = N_z = 0$ for the magnetic field parallel to the surface, therein the simulated anistropic field Ha ≈ -379.7 G, with $M \approx 1255.7$ G.

For cobalt films inherited with a higher anisotropic field, the occurrence of the coexistence of FMR and MSMR at low fields is much serious, we inevitably to exploit the equivalent *RLC* circuits to delineate the involved spectra. The equivalent circuits as shown in Fig. 7 include three parts, which composed of (A) the FMR occurring in the main straight line perpendicular to the magnetic field in which the equivalent circuit is a series resonator connected in parallel to the system impedance Z_{in}, (B) the T-type microstrip structure mode resonance (MSMR) in which the equivalent circuit is a series resonator connected in parallel to the system impedance Z_{in} and is independent to the applied magnetic field, and (C) the FMR occurring in the side arm in which the equivalent circuit is a series resonator connected in parallel to the circuit (B). The circuits are redrawn in Fig. 12 where both ends of the equivalent circuit (C) are wired to be connected to the earth, it is equivalent to the circuit as shown in Fig. 12(b) in according to above discussions.

The S_{21} spectrum for the whole combination of resonators A, B, and C is shown in Fig. 13(a). To determine the equivalent electronic elements in resonators A, B, and C, we measure four independent S_{21} parameters as shown

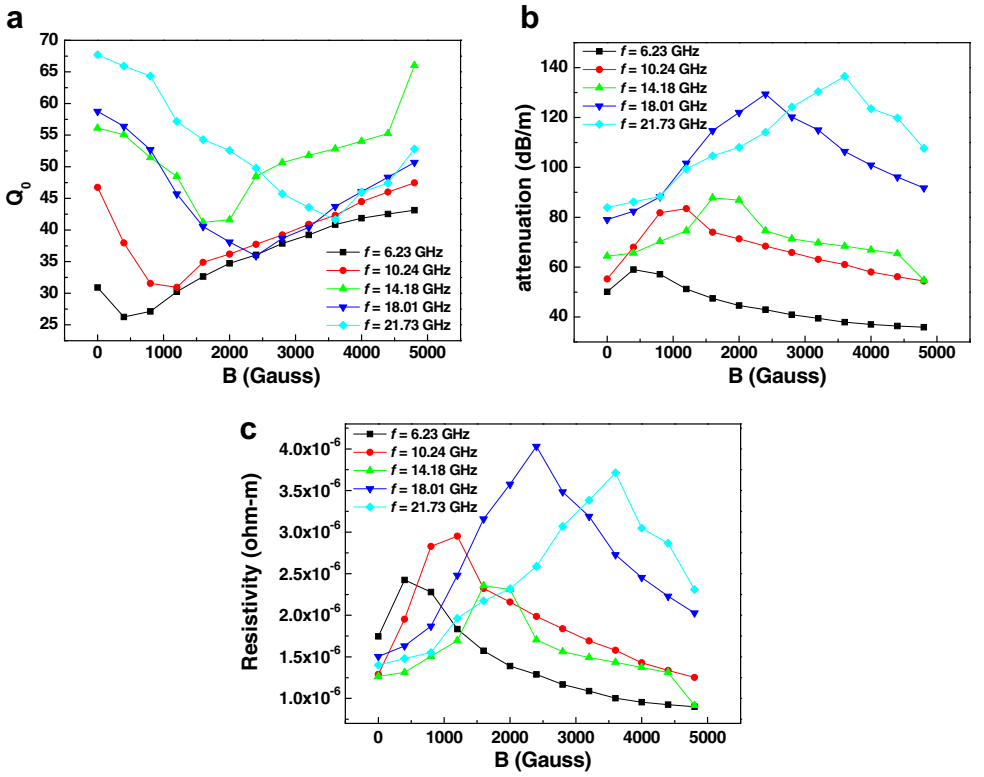

Fig. 10. The variation of the (a) *Q*-factor, (b) attenuation constant and (c) surface resistivity at various magnetic fields and resonating modes for the iron T-microstrip.

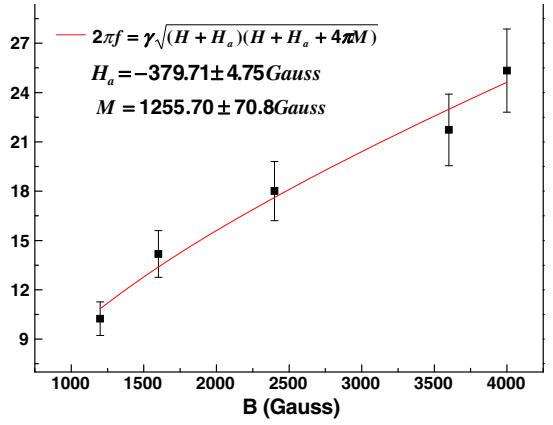

Fig. 11. The FMR peak and fitting curve of a iron T-microstrip under an applied magnetic field parallel to the iron film.

in Fig. 13 in which (a) represents the total spectrum including the resonance of A, B, and C, (b) represents the resonator A for the main straight line for the pure FMR at 2000 G, (c) describes the pure T-type MSMR of the same structure constructed by a non-magnetic copper which is barely equivalent to the resonator B, and (d) represents the pure FMR as resonator C deduced from (a) by (b) and (c). We have first tried to obtain the pure FMR by subtracting spectra (d) from (a).

We observed that the apparent MSMR resonance frequency for cobalt T-microstrip varies with the applied magnetic field in a loop of counter-clockwise directions as shown in Fig. 14 attributing to the effect of ferromagnetic absorption. For a parallel resonator as represented by a FMR, the input impedance becomes largest at the resonance frequency wherein the total impedance of the MSMR (circuit B) and the FMR (circuit C) is the largest and the transmission coefficient S_{21} will be at the highest point D as shown in Fig. 14. The equivalent impedance of FMR increases and then decreases as the applied magnetic field increases around the central resonance frequency in counter-clockwise behavior as addressed in Fig. 14. The resonance frequency related to the point D determines the equivalent *RLC* of circuit B. This can also be expressed by the following impedance variations. The FMR frequency increases with the applied magnetic field resulting in a decrease of the inductance and the capacitance in the equivalent circuits. The values of capacitance and inductance of circuit C should be equalized from parallel to series in affecting the MSMR with the same result. This equalization process means the parallel circuit is composed of the previously evaluated impedance and the inverse of impedance (or X// $(1/X)$). Coincidently, the effect of the equivalent series inductance of circuit C to the MSMR frequency reduces at first and then becomes remarkable and diminishes, and finally approaches to a constant as the field increases.

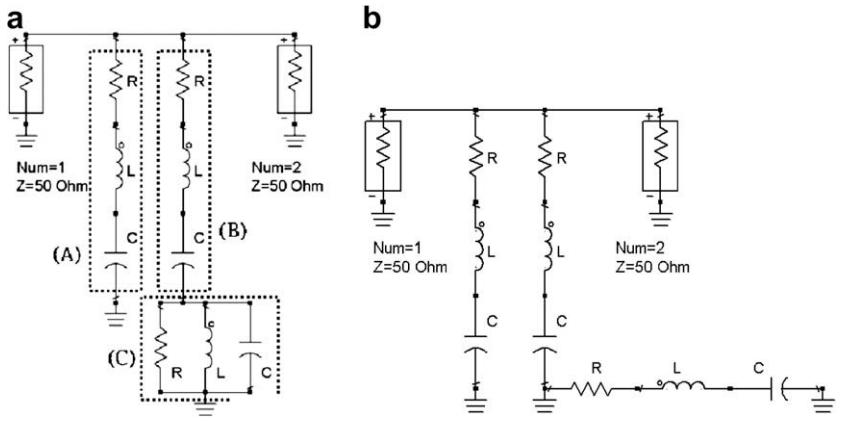

Fig. 12. (a) Equivalent circuits for three resonators and (b) equalization of (a).

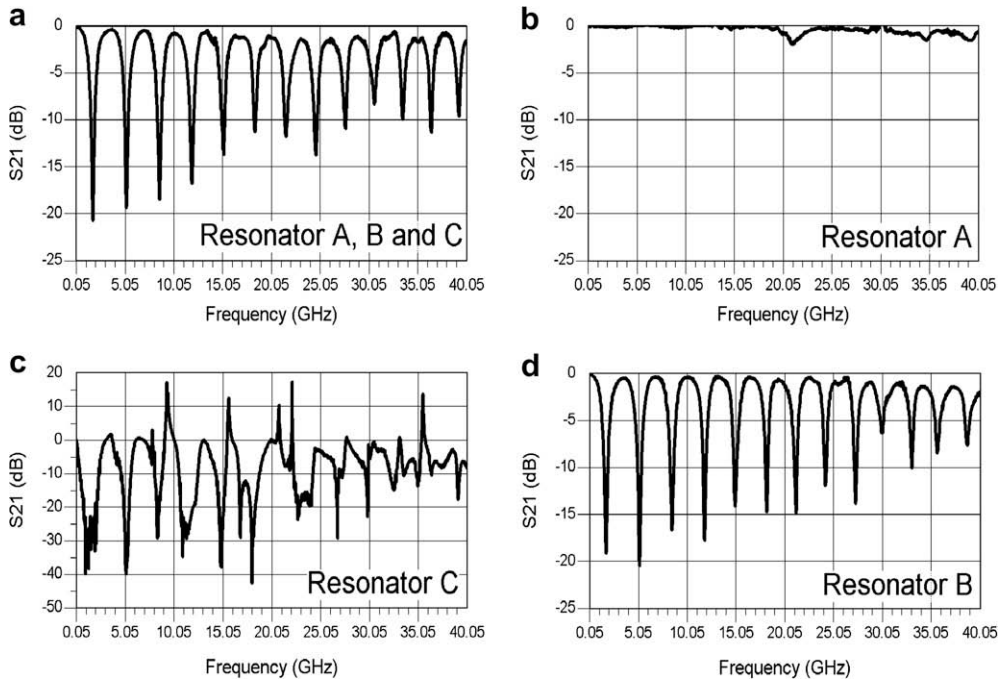

Fig. 13. The measured S_{21} spectra of the total and equivalent circuits of A, B, and C, respectively.

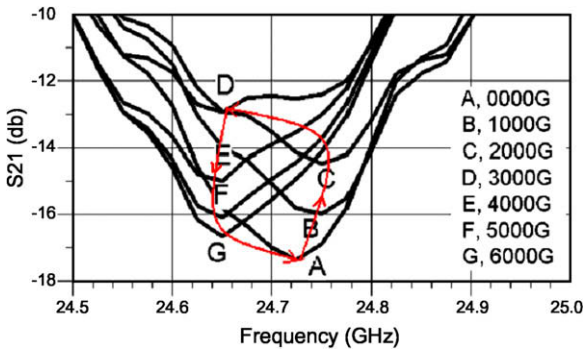

Fig. 14. The co-resonance frequency changes from A to B to C to D to E to F then to G in counter-clockwise rotation as the applied field magnetic field increases. The frequency at maximum transmission coefficient S_{21} occurs at point D corresponding to the exact FMR.

The true equivalent elements are practically solved by implementing a software entitled: Advanced Design System 2002C (Ees of EDA) designed by Agilent Technologies (USA). Within the frequency range of 0.0540 GHz there are 13 MSMR spectrum lines, the *RLC* elements (labeled 1–14) in circuits B are estimated by the corresponding resonance frequencies and *Q* factors and then the software simulates the *RLC* (labeled 15) in circuit C for this FMR resonance. As shown in Fig. 15, the simulated R15, L15, and C15 of the FMR resonator depend on the applied magnetic field. The calculated FMR frequency at different magnetic field for cobalt T-microstrip is plotted in Fig. 16 by the simulated electronic circuits. The linear plot can be fitted with Eq. (3) to solve the anisotropic field H_a and the saturation magnetization M_s.

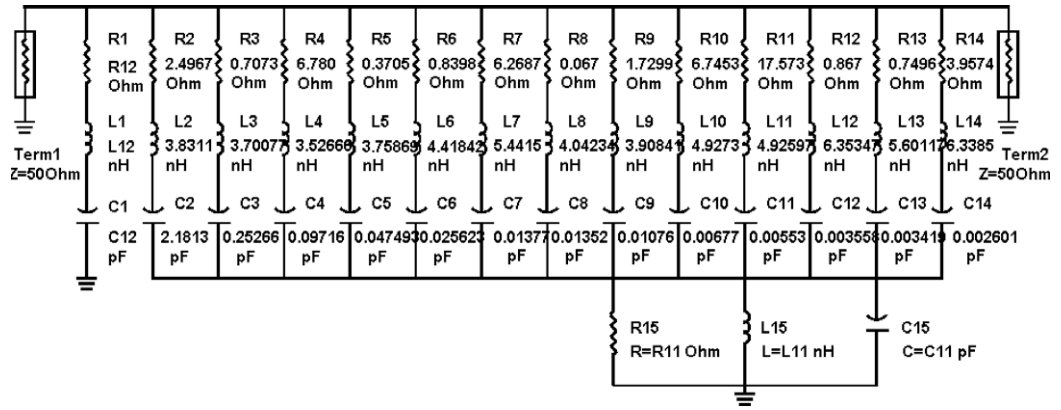

Fig. 15. Simulated 13 equivalent *RLC* (labeled from 2 to 14) to the MSMR within 0.05–40 GHz with the applied field beyond FMR (at $H = 1.45$ T), The *RLC* (labeled 15) are simulated from the results at point D in Fig. 14.

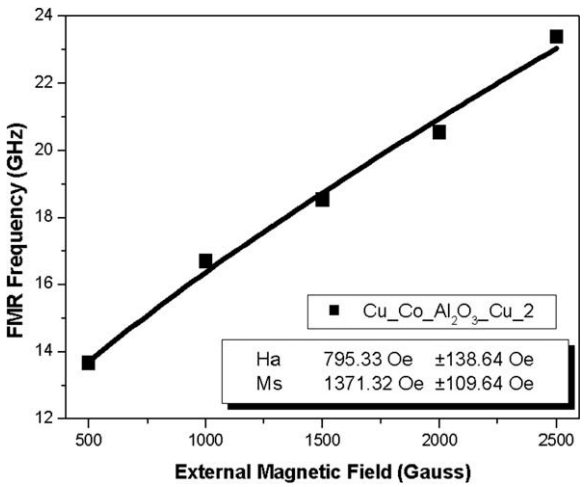

Fig. 16. The magnetic field dependence on FMR frequencies for Co T-microstrip.

5. Conclusions

The coexistence of FMR and the MSMR of a T-type transmission line observed in this experiment sugests us to determine the electric and magnetic properties simultaneously resulting from the same transmission spectra. This method eliminates the complex design of a conventional cavity to study the FMR of magnetic thin films. The equivalent *RLC* circuits of the MSMR and FMR alleviate errors introduced by the neglecting of FMR occurring at zero applied magnetic fields. With the simulated *RLC* elements, the plot of the real FMR frequency versus magnetic fields illustrates a more accurate determination of the physical constants of magnetic films.

Acknowledgement

This work was supported from the National Science Council under Contract No. NSC 97-2112-M-007-015.

References

[1] T.C. Edwards, Foundations for Microstrip Circuit Design, John Wiley and Sons, New York, 1983.
[2] H.T. Lue, J.T. Lue, T.Y. Tseng, IEEE Trans. Instrum. Meas. 51 (2002) 433.
[3] J.H. Liu, Y.C. Lin, J.T. Lue, C.J. Wu, Meas. Sci. Technol. 13 (2002) 1132.
[4] L. Bonalde, B.D. Yanoff, M.B. Salamon, D.J. Harlingen, E.M. Chia, Z.Q. Mao, Y. Macno, Phys. Rev. Lett. 85 (2000) 4775.
[5] N. Cramer, D. Lucic, R.E. Camley, Z. Celinski, J. Appl. Phys. 87 (2000) 6911.
[6] M. Tsutsumi, S. Tamura, IEEE Trans. Microw. Theory Tech. 40 (1992) 400–402.
[7] D. Spenato, A. Fessant, J. Gieraltowski, J. Loaec, H. Legall, J. Magn. Magn. Mater. 140 (1995) 1979.
[8] N. Vukadinovic, M. Labrune, J. Ben Youssef, A. Marty, J.C. Toussaint, H. Le Gall, Phys. Rev. B 65 (2002) 54403.
[9] S.W. Chang, J.H. Liu, J.T. Lue, Meas. Sci. Technol. 14 (2003) 83.
[10] C.T. Hsieh, J.Q. Lin, J.T. Lue, Appl. Surf. Sci. 252 (2005) 1899.
[11] H.A. Wheeler, IEEE Trans. Microw. Theory Tech. 25 (1977) 631.
[12] W.J. Getsinger, IEEE Trans. Microw. Theory Tech. 21 (1973) 34.
[13] M. Kirschinig, R.H. Jansen, N.H.L. Koster, Electron. Lett. 17 (1981) 123.